Article:
Huntul, MJ, Lesnic, D and Hussein, MS (2017) Reconstruction of time-dependent coefficients from heat moments. Applied Mathematics and Computation, 301. pp. 233-253. ISSN 0096-3003

https://doi.org/10.1016/j.amc.2016.12.028

Reconstruction of time-dependent coefficients from heat moments

M.J. Huntul[1,2], D. Lesnic[1] and M.S.Hussein[1,3]
[1]*Department of Applied Mathematics, University of Leeds, Leeds LS2 9JT, UK*
[2]*Department of Mathematics, College of Science, Jazan University, Jazan, Saudia Arabia*
[3]*Department of Mathematics, College of Science, University of Baghdad, Baghdad, Iraq*
E-mails addresses: mmmjmh@leeds.ac.uk (M.J.Huntul), amt5ld@maths.leeds.ac.uk (D. Lesnic), mmmsh@leeds.ac.uk (M.S.Hussein).

Abstract

This paper investigates the inverse problems of simultaneous reconstruction of time-dependent thermal conductivity, convection or absorption coefficients in the parabolic heat equation governing transient heat and bio-heat thermal processes. Using initial and boundary conditions, as well as heat moments as over-determination conditions ensure that these inverse problems have a unique solution. However, the problems are still ill-posed since small errors in the input data cause large errors in the output solution. To overcome this instability we employ the Tikhonov regularization. A discussion of the choice of multiple regularization parameters is provided. The finite-difference method with the Crank-Nicolson scheme is employed as a direct solver. The resulting inverse problems are recast as nonlinear minimization problems and are solved using the *lsqnonlin* routine from the MATLAB toolbox. Numerical results are presented and discussed.

Keywords: Inverse problem; Tikhonov's regularization; heat transfer; heat moments.

1 Introduction

Simultaneous determination of several unknown physical property coefficients in heat transfer which dependent on time, space or temperature has been investigated in various studies, see e.g. [6–9, 11].

In a recent paper [6] by the authors we have investigated the inverse problems of simultaneous numerical reconstruction of time-dependent thermal conductivity and convection coefficients in a one-dimensional parabolic equation from Cauchy boundary data measurements represented by the boundary temperature and heat flux. In this paper, we investigate the reconstruction of the same coefficients, as well as of the absorption coefficient, using the measurement of the heat moments instead of the heat flux.

The paper is organized as follows: In Section 2, the mathematical of formulation of the inverse problems are reformulated and uniqueness results are stated. In Section 3, the numerical solution of the direct problem based on finite difference method with the Crank-Nicolson scheme is presented. In Section 4, the numerical approach to solve the minimization of the nonlinear Tikhonov regularization functional is presented. The numerical results for various examples are presented and discussed in Section 5. The choice of multiple regularization parameters is also addressed. Finally, conclusions are presented in Section 6.

2 Mathematical formulation

Fix the parameters $L > 0$ and $T > 0$ representing the length of a finite slab and the time duration, respectively. Denote by $\Omega_T := (0, L) \times (0, T)$ the solution domain. We consider the parabolic heat equation

$$\frac{\partial u}{\partial t}(x,t) = a(t)\frac{\partial^2 u}{\partial x^2}(x,t) + b(t)\frac{\partial u}{\partial x}(x,t) + c(t)u(x,t) + f(x,t), \quad (x,t) \in \Omega_T, \tag{1}$$

where $a > 0$, b, c and f are coefficients, and $u(x,t)$ is the temperature. For simplicity, we have assumed that the heat capacity is constant and taken to be unity. Equation (1) has to be solved subject to the initial condition

$$u(x,0) = \phi(x), \qquad 0 \le x \le L, \tag{2}$$

and the Dirichlet boundary conditions

$$u(0,t) = \mu_1(t), \quad u(L,t) = \mu_2(t), \qquad 0 \le t \le T. \tag{3}$$

If a, b, c and f are given then (1)–(3) constitue a direct Dirichlet problem for the temperature $u(x,t)$. Other outputs of interest are the heat fluxes

$$-a(t)u_x(0,t) =: q_0(t), \quad a(t)u_x(L,t) =: q_L(t), \qquad 0 \le t \le T, \tag{4}$$

and the heat moments

$$H_k(t) = \int_0^L x^k u(x,t)dx, \quad k = 0, 1, \qquad 0 \le t \le T. \tag{5}$$

However, if any of the coefficients a, b, c and/or f are not known then we are dealing with inverse coefficient identification problems.

Prior to this study, the simultaneous identification of the coefficients $a(t)$ and $b(t)$ in the problem (1)–(3) with the additional flux data (4) has been considered in [6]. In this paper, we consider the simultaneous reconstruction of the same time-dependent coefficients, as well as of $a(t)$ and $c(t)$, but from the heat moments (5) instead of the heat fluxes (4). The uniqueness of solution of these inverse problems is stated in the next two subsections.

2.1 Inverse Problem 1

Assuming that $c(t) = 0$, the inverse problem 1 (IP1) requires the simultaneous determination of the time-dependent thermal conductivity $a(t) > 0$ and the convection (or advection) coefficient $b(t)$, together with the temperature $u(x,t)$ satisfying

$$\frac{\partial u}{\partial t}(x,t) = a(t)\frac{\partial^2 u}{\partial x^2}(x,t) + b(t)\frac{\partial u}{\partial x}(x,t) + f(x,t), \quad (x,t) \in \Omega_T, \tag{6}$$

subject to (2), (3) and (5).

The uniqueness of solution $(a(t), b(t), u(x,t))$ of this inverse problem was established in [13] and reads as follows.

Theorem 1. *Let $\phi \in C^1[0,L]$, $\mu_k \in C^1[0,T]$, $H_k \in C^1[0,T]$ for $k=0,1$, and $f \in C(\overline{\Omega_T})$. Suppose that the following condition is satisfied:*

$$U_1(t) := \Big(\mu_2(t) - \mu_1(t)\Big)\int_0^L xf(x,t)dx - \Big(L\mu_2(t) - H_0(t)\Big)\int_0^L f(x,t)dx \neq 0, \quad \forall t \in [0,T]. \tag{7}$$

Then a solution $(a(t), b(t), u(x,t)) \in C[0,T] \times C[0,T] \times \Big(C^{2,1}(\Omega_T) \cap C(\overline{\Omega_T})\Big)$ with $a(t) > 0$ for $t \in [0,T]$, to the problem (2), (3), (5) and (6) is unique.

Remark 1. Observe that by multiplying equation (6) by $x^k, k = 0, 1$, integrating with respect to x from 0 to L, and taking into account condition (5), we obtain,
$H_0'(t) = a(t)\Big(u_x(L,t) - u_x(0,t)\Big) + b(t)\Big(u(L,t) - u(0,t)\Big) + \int_0^L f(x,t)dx,$
$H_1'(t) = a(t)\Big(Lu_x(L,t) - u(L,t) + u(0,t)\Big) + b(t)\Big(Lu(L,t) - H_0(t)\Big) + \int_0^L xf(x,t)dx.$
Taking $t = 0$ in these equations, using the compatibility conditions $u_x(0,t) = \phi'(0)$, $u_x(L,t) = \phi'(L)$, the Dirichlet boundary conditions (3) and solving for $a(0)$ and $b(0)$, we obtain,

$$a(0) = \Big(\Delta(0)\Big)^{-1}\Bigg[\Big(H_0'(0) - \int_0^L f(x,0)dx\Big)\Big(L\mu_2(L) - H_0(0)\Big) - \Big(\mu_2(L) - \mu_1(0)\Big)\Big(H_1'(0) - \int_0^L xf(x,0)dx\Big)\Bigg],$$

$$b(0) = \Big(\Delta(0)\Big)^{-1}\Bigg[\Big(\phi'(L) - \phi'(0)\Big)\Big(H_1'(0) - \int_0^L xf(x,0)dx\Big) - \Big(H_0'(0) - \int_0^L f(x,0)dx\Big)\Big(L\phi'(L) - \mu_2(L) + \mu_1(0)\Big)\Bigg], \tag{8}$$

where
$\Delta(0) = \Big(\mu_2(L) - \mu_1(0)\Big)^2 + L\Big(\phi'(L)\mu_1(0) - \phi'(0)\mu_2(L)\Big) - H_0(0)\Big(\phi'(L) - \phi'(0)\Big).$

2.2 Inverse Problem 2

Assuming that $b(t) = 0$, the inverse problem 2 (IP2) requires the simultaneous determination of the time-dependent thermal conductivity $a(t) > 0$ and the absorption coefficient $c(t)$, together with the temperature $u(x,t)$ satisfying

$$\frac{\partial u}{\partial t}(x,t) = a(t)\frac{\partial^2 u}{\partial x^2}(x,t) + c(t)u(x,t) + f(x,t), \quad (x,t) \in \Omega_T, \tag{9}$$

subject to (2), (3) and (5). In bio-heat transfer, equation (9) is known as the Pennes bio-heat equation and $c(t)$ represents the perfusion coefficient, [15]. In case where the thermal conductivity coefficient $a(t)$ is known, and taken to be unity, the inverse problem (2), (3), (9) with the the integral condition (5) for $k = 0$, for recovering the perfusion coefficient $c(t)$ and the temperature $u(x,t)$ was studied both theoretically and numerically

in [2] and [15], respectively.

The uniqueness of solution $(a(t), c(t), u(x,t))$ of the IP2 was established in [8] and reads as follows.

Theorem 2. *Let $\phi \in C^1[0,L]$, $\mu_k \in C[0,T]$, $H_k \in C^1[0,T]$ for $k=0,1$, and $f \in C(\overline{\Omega_T})$. Suppose that the following condition is satisfied:*

$$U_2(t) := H_0(t)H_1^{'}(t) - H_0^{'}(t)H_1(t) + \int_0^L \Big(H_1(t) - xH_0(t)f(x,t)\Big)dx \neq 0, \quad \forall t \in [0,T]. \tag{10}$$

Then a solution $(a(t), c(t), u(x,t)) \in C[0,T] \times C[0,T] \times \Big(C^{2,1}(\Omega_T) \cap C^{1,0}(\overline{\Omega_T})\Big)$ with $a(t) > 0$ for $t \in [0,T]$, to the problem (2), (3), (5) and (9) is unique.

Remark 2. Observe that by multiplying equation (8) by $x^k, k=0,1$, integrating with respect to x from 0 to L, and taking into account condition (5), we obtain, [8],
$H_0'(t) = a(t)\Big(u_x(L,t) - u_x(0,t)\Big) + c(t)H_0(t) + \int_0^L f(x,t)dx,$
$H_1'(t) = a(t)\Big(Lu_x(L,t) - u(L,t) + u(0,t)\Big) + c(t)H_1(t) + \int_0^L xf(x,t)dx.$
As before in Remark 1, taking $t=0$ in these equations and solving for $a(0)$ and $c(0)$, we obtain,

$$a(0) = \Big(\Theta(0)\Big)^{-1}\left[H_1(0)\Big(H_0'(0) - \int_0^L f(x,0)dx\Big) - H_0(0)\Big(H_1'(0) - \int_0^L xf(x,0)dx\Big)\right],$$

$$c(0) = \Big(\Theta(0)\Big)^{-1}\left[\Big(H_1'(0) - \int_0^L xf(x,0)dx\Big)\Big(\phi'(L) - \phi'(0)\Big) - \Big(H_0'(0) - \int_0^L f(x,0)dx\Big)\Big(L\phi'(L) - \mu_2(L) + \mu_1(0)\Big)\right], \tag{11}$$

where
$\Theta(0) = H_1(0)\Big(\phi'(L) - \phi'(0)\Big) - H_0(0)\Big(L\phi'(L) - \mu_2(L) + \mu_1(0)\Big).$

3 Numerical solution of direct problem

In this section, we consider the direct initial boundary value problem given by equations (1)–(3). We use the finite-difference method (FDM) with the Crank-Nicholson scheme, [14], which is unconditionally stable and second-order accurate in space and time. We denote $u(x_i,t_j) = u_{i,j}$, $a(t_j) = a_j$, $b(t_j) = b_j$, $c(t_j) = c_j$ and $f(x_i,t_j) = f_{i,j}$, where $x_i = i\Delta x$, $t_j = j\Delta t$ for $i = \overline{0,M}$, $j = \overline{0,N}$, and $\Delta x = \frac{L}{M}$, $\Delta t = \frac{T}{N}$.

Considering the general partial differential equation

$$u_t = G(x,t,u,u_x,u_{xx}), \tag{12}$$

the Crank-Nicolson method, [14], discretises (12), (2) and (3) as

$$\frac{u_{i,j+1} - u_{i,j}}{\Delta t} = \frac{1}{2}(G_{i,j} + G_{i,j+1}), \quad i = \overline{1,(M-1)},\ j = \overline{0,(N-1)}, \tag{13}$$

$$u_{i,0} = \phi(x_i), \qquad i = \overline{0, M}, \tag{14}$$

$$u_{0,j} = \mu_1(t_j), \quad u_{M,j} = \mu_2(t_j), \qquad j = \overline{0, N}, \tag{15}$$

where

$$G_{i,j} = G\Big(x_i, t_j, u_{i,j}, \frac{u_{i+1,j} - u_{i-1,j}}{2(\Delta x)}, \frac{u_{i+1,j} - 2u_{i,j} + u_{i-1,j}}{(\Delta x)^2}\Big),$$

$$G_{i,j+1} = G\Big(x_i, t_{j+1}, u_{i,j+1}, \frac{u_{i+1,j+1} - u_{i-1,j+1}}{2(\Delta x)}, \frac{u_{i+1,j+1} - 2u_{i,j+1} + u_{i-1,j+1}}{(\Delta x)^2}\Big),$$

$$i = \overline{1, (M-1)}, j = \overline{0, (N-1)}. \tag{16}$$

For our problem, equation (1) can be discretised in the form of (12) as

$$-A_{j+1}u_{i-1,j+1} + (1 + B_{j+1})u_{i,j+1} - C_{j+1}u_{i+1,j+1} =$$

$$A_j u_{i-1,j} + (1 - B_j)u_{i,j} + C_j u_{i+1,j} + \frac{\Delta t}{2}(f_{i,j} + f_{i,j+1}), \tag{17}$$

for $i = \overline{1, (M-1)}$, $j = \overline{0, (N-1)}$, where
$A_j = \dfrac{(\Delta t)a_j}{2(\Delta x)^2} - \dfrac{(\Delta t)b_j}{4(\Delta x)}$, $B_j = \dfrac{(\Delta t)a_j}{(\Delta x)^2} - \dfrac{(\Delta t)c_j}{2}$, $C_j = \dfrac{(\Delta t)a_j}{2(\Delta x)^2} + \dfrac{(\Delta t)b_j}{4(\Delta x)}$.

At each time step t_{j+1}, for $j = \overline{0, (N-1)}$, using the Dirichlet boundary conditions (15), the above difference equation can be reformulated as a $(M-1) \times (M-1)$ system of linear equations of the form,

$$D\mathbf{u_{j+1}} = E\mathbf{u_j} + \mathbf{b}, \tag{18}$$

where

$$\mathbf{u_{j+1}} = (u_{1,j+1}, u_{2,j+1}, ..., u_{M-2,j+1}, u_{M-1,j+1})^{\mathrm{T}},$$

$$D = \begin{pmatrix} 1 + B_{j+1} & -C_{j+1} & 0 & ... & 0 & 0 & 0 \\ -A_{j+1} & 1 + B_{j+1} & -C_{j+1} & ... & 0 & 0 & 0 \\ \vdots & \vdots & \vdots & \ddots & \vdots & \vdots & \vdots \\ 0 & 0 & 0 & ... & -A_{j+1} & 1 + B_{j+1} & -C_{j+1} \\ 0 & 0 & 0 & ... & 0 & -A_{j+1} & 1 + B_{j+1} \end{pmatrix},$$

$$E = \begin{pmatrix} 1 - B_j & C_j & 0 & ... & 0 & 0 & 0 \\ A_j & 1 - B_j & C_j & ... & 0 & 0 & 0 \\ \vdots & \vdots & \vdots & \ddots & \vdots & \vdots & \vdots \\ 0 & 0 & 0 & ... & A_j & 1 - B_j & C_j \\ 0 & 0 & 0 & ... & 0 & A_j & 1 - B_j \end{pmatrix},$$

and

$$\mathbf{b} = \begin{pmatrix} \frac{\Delta t}{2}(f_{1,j} + f_{1,j+1}) + A_j\mu_1(t_j) + A_{j+1}\mu_1(t_{j+1}) \\ \frac{\Delta t}{2}(f_{2,j} + f_{2,j+1}) \\ \vdots \\ \frac{\Delta t}{2}(f_{M-2,j} + f_{M-2,j+1}) \\ \frac{\Delta t}{2}(f_{M-1,j} + f_{M-1,j+1}) + C_j\mu_2(t_j) + C_{j+1}\mu_2(t_{j+1}) \end{pmatrix}.$$

As an example, consider the direct problem (1)–(3) with $T = L = 1$,

$$c(t) = 0, \quad \phi(x) = u(x,0) = e^{-x} + x^2, \quad \mu_1(t) = u(0,t) = e^t,$$
$$\mu_2(t) = u(1,t) = (e^{-1}+1)e^t, \; f(x,t) = e^t\Big((1+t)e^{-x} + x^2 - 2(1+t) - 2x(1+2t)\Big), \quad (19)$$

and

$$a(t) = 1 + t, \quad b(t) = 1 + 2t. \quad (20)$$

The exact solution is given by

$$u(x,t) = (e^{-x} + x^2)e^t. \quad (21)$$

The numerical results for the interior temperature $u(x,t)$ have been obtained in excellent agreement with the exact solution (21) and therefore they are not presented.

Apart from the interior temperature $u(x,t)$, other outputs of interest are the heat fluxes in equation (4) and the heat moments in equation (5) over the time interval $[0,T]$, which analytically are given by

$$q_0(t) = -a(t)u_x(0,t) = (1+t)e^t, \qquad t \in [0,1], \quad (22)$$

$$q_1(t) = a(t)u_x(1,t) = (1+t)(2-e^{-1})e^t, \qquad t \in [0,1], \quad (23)$$

$$H_0(t) = \int_0^1 e^t(e^{-x} + x^2)dx = e^t\Big(-e^{-1} + \frac{4}{3}\Big), \qquad t \in [0,1], \quad (24)$$

$$H_1(t) = \int_0^1 xe^t(e^{-x} + x^2)dx = e^t\Big(-2e^{-1} + \frac{5}{4}\Big), \qquad t \in [0,1]. \quad (25)$$

Figure 1 shows that the exact and numerical solutions for the heat fluxes (4) and heat moments (5) are indistinguishable. The exact solutions are given in equations (22)–(25), whilst the numerical solutions have been calculated using the following $O((\Delta x)^2)$ finite-difference approximation and trapezoidal rule formulas:

$$q_0(t_j) = -a(t_j)u_x(0,t_j) = -\frac{(4u_{1,j} - u_{2,j} - 3\mu_1(t_j))a_j}{2\Delta x}, \; j = \overline{0,N}, \quad (26)$$

$$q_1(t_j) = a(t_j)u_x(1,t_j) = -\frac{(4u_{M-1,j} - u_{M-2,j} - 3\mu_2(t_j))a_j}{2\Delta x}, \; j = \overline{0,N}, \quad (27)$$

and

$$H_k(t_j) = \int_0^1 x^k u(x,t_j)dx = \frac{1}{2N}\Big(x_0^k u_{0,j} + x_M^k u_{M,j} + \sum_{i=1}^{M-1} x_i^k u_{i,j}\Big), \; k = 0,1, j = \overline{0,N}, \quad (28)$$

with the convention that $x_0^0 = 1$. Note that for $j = 0$ in (24) and (25), using (2) and (5), we obtain,

$$H_k(0) = \int_0^1 x^k u(x,0)dx = \frac{1}{2N}\Big(x_0^k\phi(x_0) + x_M^k\phi(x_M) + \sum_{i=1}^{M-1} x_i^k\phi(x_i)\Big), \quad k = 0,1. \quad (29)$$

(a)

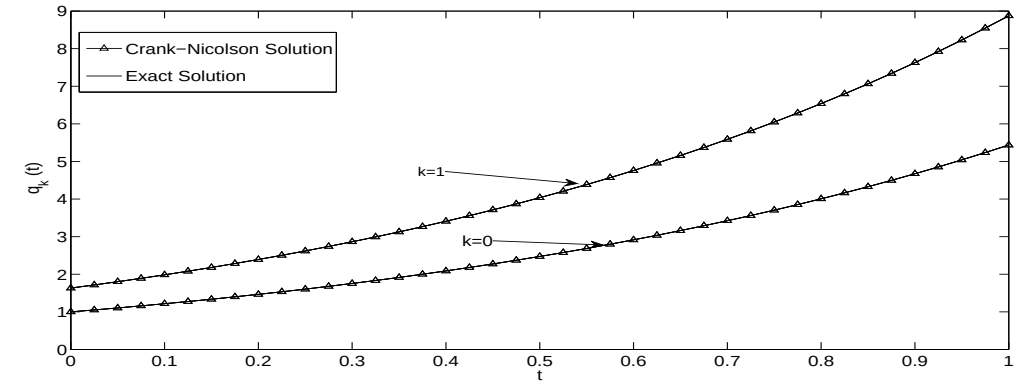

(b)

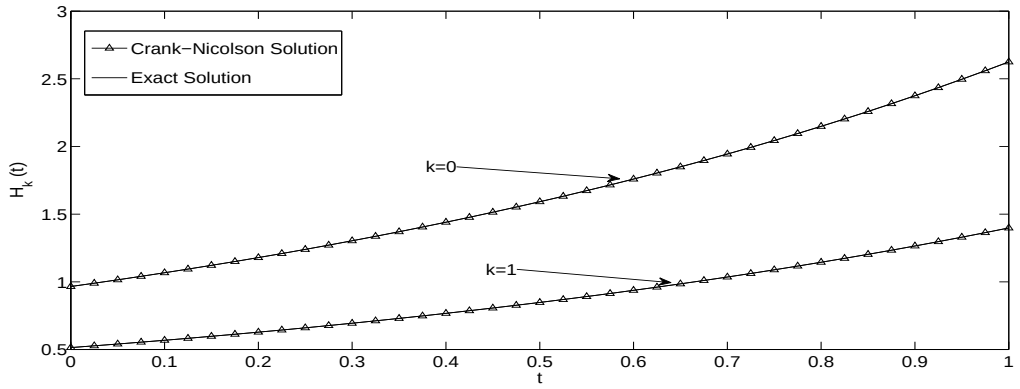

Figure 1: The exact and the numerical (a) heat fluxes $q_k(t)$ and (b) heat moments $H_k(t)$, $k = 0, 1$, for $M = N = 40$, for the direct problem.

The root means square errors $(rmse)$ between the numerical and exact solutions for heat fluxes and heat moments (4) and (5) are shown in Table 1. These have been calculated using the formulas

$$rmse(q_k) := \sqrt{\frac{1}{N}\sum_{j=1}^{N}(q_k^{numerical}(t_j) - q_k^{exact}(t_j))^2}, \quad k = 0, 1, \tag{30}$$

$$rmse(H_k) := \sqrt{\frac{1}{N}\sum_{j=1}^{N}(H_k^{numerical}(t_j) - H_k^{exact}(t_j))^2}, \quad k = 0, 1. \tag{31}$$

From Table 1 it can be seen that the $(rmse)$ (30) and (31) decrease, as $M = N$ increase. They also confirm that the error is of $O((\Delta x)^2)$.

Table 1: The ($rmse$) given by equtions (30) and (31) between the exact and numerical solutions for the heat fluxes and heat moments, for $M = N \in \{10, 20, 40\}$, for the direct problem.

$M = N$	10	20	40
$rmse(q_0)$	0.0089	0.0022	0.0005
$rmse(q_1)$	0.0046	0.0011	0.0002
$rmse(H_0)$	0.0041	0.0009	0.0002
$rmse(H_1)$	0.0031	0.0007	0.0001

4 Numerical approach to solve the inverse problem

In the inverse problems, we assume that the coefficients $a(t)$, $b(t)$ or $c(t)$ are unknown. Usually, the nonlinear inverse problem can be formulated as a nonlinear least-squares minimization. The regularized objective function which is minimized is given by

$$F(a,b) = \Big\| \int_0^1 u(x,t)dx - H_0(t) \Big\|^2 + \Big\| \int_0^1 xu(x,t)dx - H_1(t) \Big\|^2 + \beta_1 \Big\| a(t) \Big\|^2 + \beta_2 \Big\| b(t) \Big\|^2, \tag{32}$$

or

$$F(a,c) = \Big\| \int_0^1 u(x,t)dx - H_0(t) \Big\|^2 + \Big\| \int_0^1 xu(x,t)dx - H_1(t) \Big\|^2 + \beta_1 \Big\| a(t) \Big\|^2 + \beta_2 \Big\| c(t) \Big\|^2, \tag{33}$$

where u solves (2), (3) and (6) or (9) for given (a, b) or (a, c), respectively, $\beta_1, \beta_2 \geq 0$ are regularization parameters and the norm is usually the $L^2[0, T]$-norm. The discretizations of (32) and (33) are:

$$F(\mathbf{a},\mathbf{b}) = \sum_{j=1}^{N} \Big[\int_0^1 u(x,t_j)dx - H_0(t_j) \Big]^2 + \sum_{j=1}^{N} \Big[\int_0^1 xu(x,t_j)dx - H_1(t_j) \Big]^2 + \beta_1 \sum_{j=1}^{N} a_j^2 + \beta_2 \sum_{j=1}^{N} b_j^2. \tag{34}$$

and

$$F(\mathbf{a},\mathbf{c}) = \sum_{j=1}^{N} \Big[\int_0^1 u(x,t_j)dx - H_0(t_j) \Big]^2 + \sum_{j=1}^{N} \Big[\int_0^1 xu(x,t_j)dx - H_1(t_j) \Big]^2 + \beta_1 \sum_{j=1}^{N} a_j^2 + \beta_2 \sum_{j=1}^{N} c_j^2. \tag{35}$$

The case $\beta_1 = \beta_2 = 0$ yields the ordinary nonlinear least-squares method which is usually unstable. The minimization of F subject to the physical constraints $\mathbf{a} > \mathbf{0}$ is accomplished using the MATLAB toolbox routine *lsqnonlin*, [12]. This routine finds the minimum of the sum of squares of functions starting from an initial guess and is based on the Trust-Region-Reflection algorithm, [3].

We take the parameters of the routine as follows:

- Number of variables $M = N = 40$.
- xTolerance (xTol) = 10^{-30}.
- Function Tolerance (FunTol) = 10^{-30}.
- Initial guess $(\mathbf{a}^{(0)}, \mathbf{b}^{(0)}) = (\mathbf{a}(0), \mathbf{b}(0))$ for IP1 and $(\mathbf{a}^{(0)}, \mathbf{c}^{(0)}) = (\mathbf{a}(0), \mathbf{c}(0))$ for IP2. The values of $a(0)$, $b(0)$ and $c(0)$ are calculated from equations (8) and (11).
- The lower and upper simple bounds are 10^{-10} and 10^3 for a, and -10^3 and 10^3 for b and c.

5 Numerical results and discussion

In this section, we discuss a few test examples to illustrate the accuracy and stability of the numerical solutions. We take $T = L = 1$. We investigate the cases when the coefficients $a(t)$, $b(t)$ or $c(t)$ are smooth and non-smooth. In addition, we add noise to the measured heat moments input data (5) as

$$H_k^{noise}(t_j) = H_k(t_j) + \epsilon_k^j, \quad k = 0, 1, \quad j = \overline{1, N}, \tag{36}$$

where ϵ_k^j are random variable generated from a Gaussian normal distribution with mean zero and standard deviations σ_k, given by

$$\sigma_k = p \times \max_{t\in[0,T]} |H_k(t)|, \quad k = 0, 1, \tag{37}$$

where p represents the percentage of noise. We use the MATLAB function *normrnd* to generate the random variables as

$$\boldsymbol{\epsilon}_k = normrnd(0, \sigma, N), \quad k = 0, 1. \tag{38}$$

The root mean square error ($rmse$) to analyse the error between the exact and estimated coefficients, is defined as,

$$rmse(a(t)) = \sqrt{\frac{1}{N}\sum_{j=1}^{N}\left(a^{numerical}(t_j) - a^{exact}(t_j)\right)^2}, \tag{39}$$

and similar expressions exist for $b(t)$ and $c(t)$.

Example 1 (for IP1)

Consider the IP1 given by equations (2), (3), (5) and (6) with unknown coefficients $a(t)$, $b(t)$ and solve this inverse problem with the input data (19), (24) and (25). The graph of the function $U_1(t)$ given by equation (7) is shown in Figure 2. From this figure it can be seen that this function never vanishes over the time interval $t \in [0, 1]$ and hence condition (7) is satisfied. Consequently, according to Theorem 1, a solution to the IP1 given by equations (2), (3), (5) and (6) with data (19), (24) and (25) is unique. In fact, it can easily be verified by direct substitution that the solution $(a(t), b(t), u(x, t))$ is given by equations (20) and (21). Note also that the direct problem (1)–(3) associated to this

example has been previously solved numerically using the FDM in Section 3.

First, we consider that there is no noise in the input data (5). The unregularized objective function (34), i.e. with $\beta_1 = \beta_2 = 0$, as a function of the number of iterations, is shown in Figure 3. From this figure it can be seen that it decreases rapidly to a very low value of $O(10^{-28})$ in 20 iterations. The numerical results for the corresponding coefficients $a(t)$ and $b(t)$ are presented in Figure 4. From this figure it can be seen that the retrieved coefficients are in very good agreement with the exact solution (20).

Next, we add $p = 1\%$ noise to the heat moments $H_0(t)$ and $H_1(t)$, as given by equation (36). Taking first $\beta_1 = \beta_2$, the L-curve, [5], for the choice of the regularization parameter is shown in Figure 5, where the

$$\text{Residual norm} = \sqrt{\sum_{k=0}^{1} \left\| \int_0^1 x^k u(x,\cdot)dx - H_k^{noise}(\cdot) \right\|^2}. \tag{40}$$

From this figure it can be seen that the three regularization parameters near the "corner" of the L-curve are $\beta_1 = \beta_2 \in \{10^{-4}, 10^{-3}, 10^{-2}\}$. Second, allowing for independent values of β_1 and β_2 we obtain the numerical results summarised in Table 2. In this table, we have highlighted some representative choices for β_1 and β_2 with the corresponding numerical solutions for a and b plotted in Figure 6 and the absolute errors between numerical and exact solutions for u plotted in Figure 7.

We note that for the choice of the two-parameter family of regularization parameters (β_1, β_2) we have initially tried to apply the heuristic L-surface method, [1], but without success. Next, we investigate the application of the discrepancy domain principle, [4], which selects the regularization parameters (β_1, β_2) belonging to the domain

$$D(\varepsilon) = \left\{ (\beta_1, \beta_2) \in \mathbb{R}_+^2 \,\middle|\, \varepsilon < \text{Residual norm} \leq \tau\varepsilon \right\}, \tag{41}$$

for some constant $\tau > 1$ independent on β_1, β_2 and ε, where

$$\varepsilon = \varepsilon(p) = \sqrt{\sum_{k=0}^{1} \sum_{j=1}^{N} (\epsilon_k^j)^2} \tag{42}$$

represents the total amount of noise which is input in (36). For $p = 1\%$, from (42) we report $\varepsilon(1\%) = 0.2459$. By inspecting Table 2 and invoking criterion (41) one can discard choices with $\beta_1 \leq 10^{-3}$ as producing unstable solutions. Also, one can observe that the choices $\beta_1 = 10^{-2}$, $\beta_2 = 10^{-3}$ and $\beta_1 = 10^{-2}$, $\beta_2 = 10^{-2}$ satisfy criterion (41) for some $\tau > 1$, but the choice $\beta_1 = 10^{-3}$, $\beta_2 = 10^{-4}$ does not. This is consistent with the numerical results presented in Figure 6 where the numerical solution obtained with the under-regularization parameters $\beta_1 = 10^{-3}$, $\beta_2 = 10^{-4}$ is rather unstable, whilst the choice $\beta_1 = 10^{-2}$, $\beta_2 = 10^{-3}$ seems optimal.

From the above discussion and related solution [1,4,10] one can realise that the choice of multiple regularization parameters is a difficult and open topic and more research needs to be undertaken in the future. In what follows, in Examples 2–4, for simplicity, we present results obtained with some trial-and-error typical values of β_1 and β_2 which ensure that stable solutions are obtained.

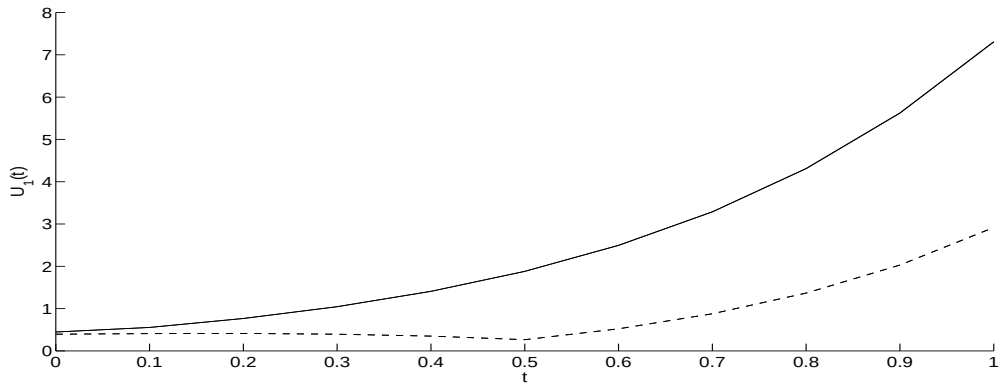

Figure 2: The graph of the function $U_1(t)$, as a function of t, given by (7) for Example 1 (——) and Example 2 (− − −).

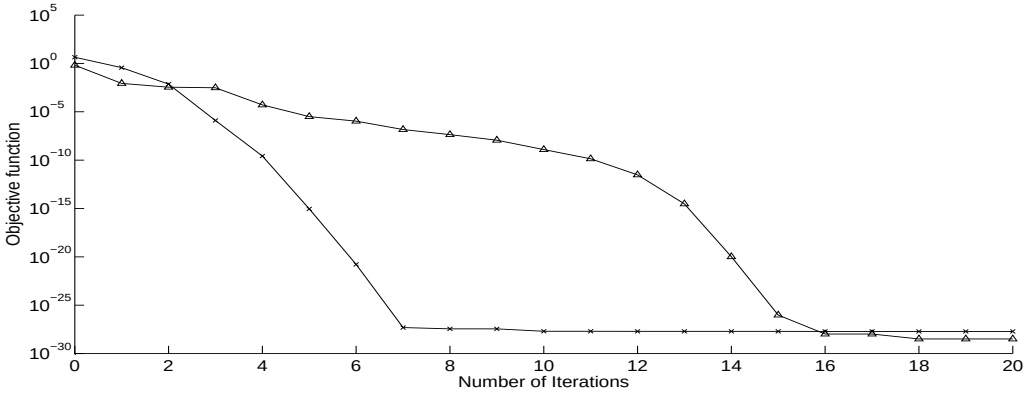

Figure 3: Objective function (34), for Example 1 (−x−) and Example 2 (−△−), with no noise and no regularization.

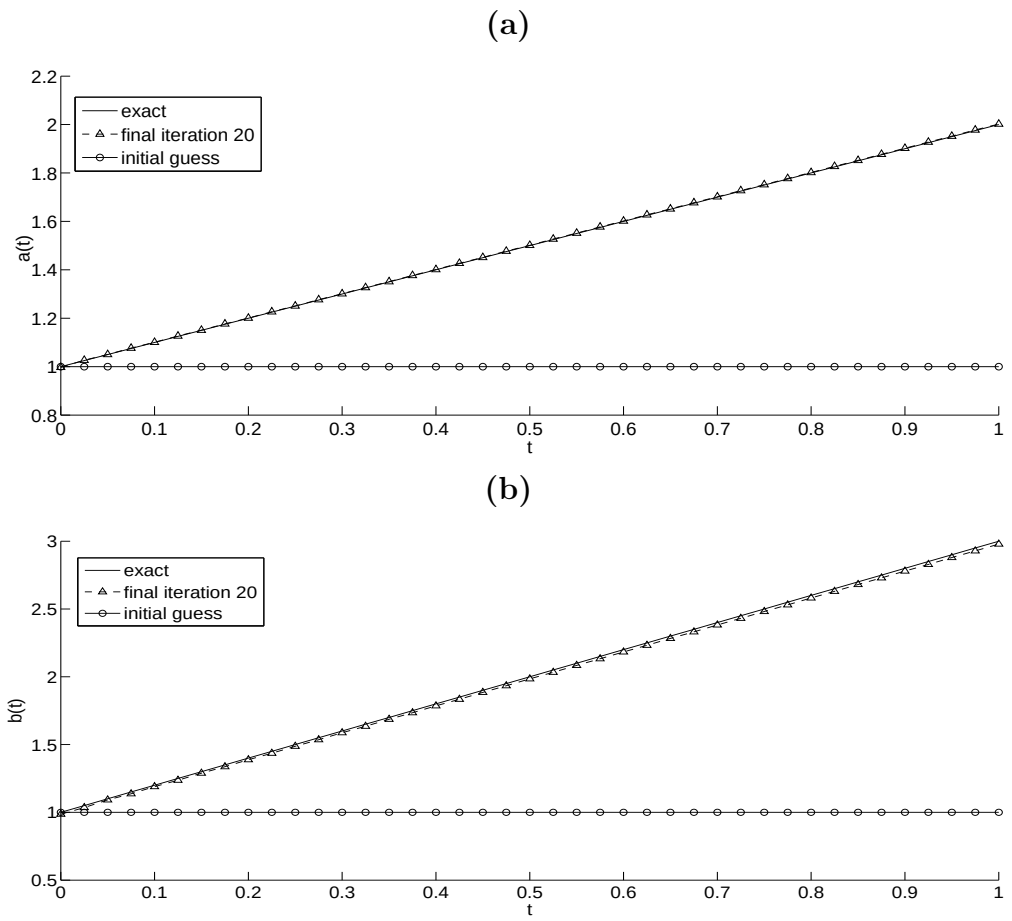

Figure 4: (a) Coefficient $a(t)$ and (b) Coefficient $b(t)$, for Example 1 with no noise and no regularization.

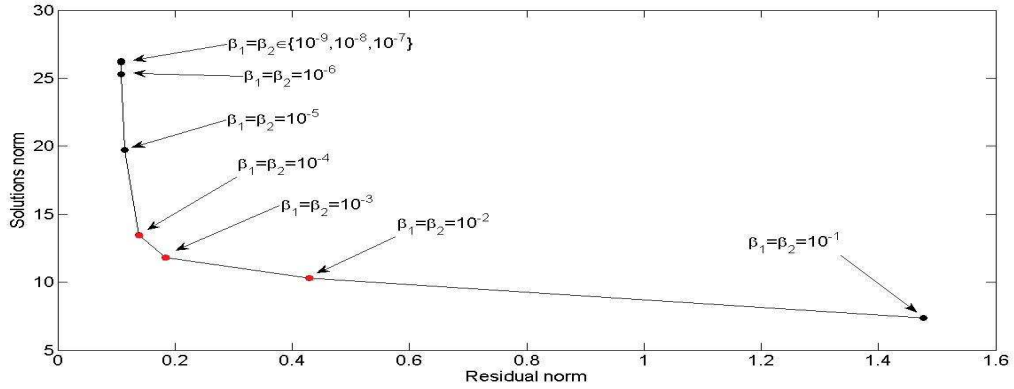

Figure 5: The residual norm (40) versus the solution norm $\sqrt{||a||^2+||b||^2}$ for the L-curve with various regularization parameters, for Example 1 with $p = 1\%$ noise.

Table 2: The objective function (34), $rmse$, residual and norms for estimated coefficients for IP1 of Example 1 with $p = 1\%$ noise and various regularization parameters.

$\beta_1 \backslash \beta_2$		10^{-9}	10^{-8}	10^{-7}	10^{-6}	10^{-5}	10^{-4}	10^{-3}	10^{-2}	10^{-1}
10^{-9}	Obj.function	0.0116	0.0116	0.0117	0.0121	0.0152	0.0193	0.0200	0.0201	0.0201
	$rmse(a)$	1.1252	1.1252	1.1253	1.1254	1.1235	1.2054	1.1365	1.1261	1.1252
	$rmse(b)$	2.8876	2.8862	2.8717	2.7267	1.7860	1.8301	2.0577	2.0829	2.0854
	Residual	0.1078	0.1078	0.1078	0.1079	0.1144	0.1359	0.1411	0.1416	0.1416
	$\|\|a\|\|$	12.199	12.201	12.211	12.303	12.941	14.207	14.087	14.062	14.060
	$\|\|b\|\|$	23.242	23.231	23.122	22.063	14.508	2.8511	0.2680	0.0265	0.0027
10^{-8}	Obj.function	0.0116	0.0116	0.0117	0.0121	0.0152	0.0193	0.0200	0.0201	0.0201
	$rmse(a)$	1.1251	1.1251	1.1253	1.1253	1.1235	1.2054	1.1364	1.1261	1.1252
	$rmse(b)$	2.8876	2.8862	2.8717	2.7268	1.7860	1.8301	2.0577	2.0829	2.0854
	Residual	0.1078	0.1078	0.1078	0.1079	0.1144	0.1359	0.1411	0.1416	0.1416
	$\|\|a\|\|$	12.199	12.200	12.211	12.302	12.941	14.207	14.087	14.062	14.060
	$\|\|b\|\|$	23.243	23.232	23.123	22.064	14.509	2.8513	0.2679	0.0265	0.0027
10^{-7}	Obj.function	0.0116	0.0116	0.0117	0.0122	0.0152	0.0193	0.0200	0.0201	0.0201
	$rmse(a)$	1.1246	1.1246	1.1248	1.1249	1.1231	1.2050	1.1354	1.1251	1.1242
	$rmse(b)$	2.8876	2.8861	2.8717	2.7265	1.7860	1.8299	2.0577	2.0829	2.0854
	Residual	0.1078	0.1078	0.1078	0.1079	0.1144	0.1359	0.1411	0.1416	0.1416
	$\|\|a\|\|$	12.196	12.197	12.208	12.299	12.939	14.205	14.083	14.058	14.056
	$\|\|b\|\|$	23.249	23.238	23.129	22.068	14.5135	2.8518	0.2678	0.0265	0.0026
10^{-6}	Obj.function	0.0118	0.0118	0.0118	0.0123	0.0154	0.0195	0.0202	0.0202	0.0203
	$rmse(a)$	1.1200	1.1201	1.1203	1.1207	1.1198	1.2016	1.1254	1.1165	1.1158
	$rmse(b)$	2.8884	2.8869	2.8723	2.7245	1.7860	1.8282	2.0576	2.0828	2.0854
	Residual	0.1078	0.1078	0.1078	0.1079	0.1143	0.1359	0.1411	0.1416	0.1416
	$\|\|a\|\|$	12.163	12.164	12.175	12.270	12.919	14.190	14.045	14.026	14.024
	$\|\|b\|\|$	23.309	23.298	23.187	22.111	14.559	2.8544	0.2665	0.0264	0.0026
10^{-5}	Obj.function	0.0131	0.0131	0.0131	0.0136	0.0168	0.0213	0.0219	0.0220	0.0220
	$rmse(a)$	1.0854	1.0854	1.0856	1.0882	1.0938	1.1446	1.0713	1.0692	1.0691
	$rmse(b)$	2.9189	2.9171	2.8995	2.7385	1.7776	1.8147	2.0565	2.0827	2.0854
	Residual	0.0856	0.1080	0.1080	0.1080	0.1139	0.1361	0.0219	0.1417	0.1417
	$\|\|a\|\|$	11.884	11.885	11.899	12.021	12.742	13.960	13.840	13.846	13.847
	$\|\|b\|\|$	23.965	23.952	23.820	22.634	15.023	2.8359	0.2641	0.0263	0.0026
10^{-4}	Obj.function	0.0236	0.0236	0.0237	0.0245	0.0297	0.0373	0.0385	0.0386	0.0386
	$rmse(a)$	0.9040	0.9039	0.9022	0.8995	0.9146	0.9100	0.9353	0.9371	0.9372
	$rmse(b)$	3.7526	3.7494	3.7169	3.3481	1.9023	1.6453	2.0384	2.0809	2.0852
	Residual	0.1175	0.1175	0.1173	0.1162	0.0297	0.1383	0.1437	0.1442	0.1442
	$\|\|a\|\|$	9.8774	9.8789	9.8940	10.067	11.154	12.972	13.322	13.353	13.356
	$\|\|b\|\|$	31.558	31.538	31.333	29.148	19.9816	3.6333	0.3591	0.0359	0.0036
10^{-3}	Obj.function	0.0581	0.0581	0.0583	0.0604	0.0756	0.1464	0.1737	0.1763	0.1766
	$rmse(a)$	0.9978	0.9977	0.9968	0.9723	0.8990	0.3452	0.4391	0.4597	0.4618
	$rmse(b)$	6.1800	6.1775	6.1525	5.4835	4.1854	0.8470	1.8259	2.0598	2.0831
	Residual	0.1996	0.1996	0.1995	0.1983	0.1929	0.1694	0.1837	0.1855	0.1857
	$\|\|a\|\|$	4.2682	4.2687	4.2743	4.3567	4.8573	9.3536	11.707	11.901	11.919
	$\|\|b\|\|$	49.073	49.059	48.924	45.311	38.438	17.384	1.7106	0.1699	0.0170
10^{-2}	Obj.function	0.0868	0.0759	0.0871	0.0931	0.1141	0.2812	1.0709	1.2397	1.2535
	$rmse(a)$	1.4304	1.4446	1.4302	1.4166	1.4087	1.3140	0.2534	0.1848	0.1923
	$rmse(b)$	7.4462	8.2955	7.4317	6.7808	5.3679	4.4335	0.4258	1.8922	2.0666
	Residual	0.2815	0.2616	0.2814	0.2865	0.2898	0.2942	0.3578	0.4285	0.4348
	$\|\|a\|\|$	0.8702	0.8629	0.8709	0.8974	0.9301	1.5236	8.4957	10.199	10.310
	$\|\|b\|\|$	57.551	62.8293	57.469	53.806	46.3387	41.400	14.869	1.2524	0.1231
10^{-1}	Obj.function	0.0586	0.0738	0.0722	0.0719	0.0863	0.3054	1.8226	7.0848	7.5868
	$rmse(a)$	1.5163	1.5173	1.5159	1.5123	1.5217	1.5044	1.4064	0.5129	0.4327
	$rmse(b)$	9.9355	9.0484	8.8824	8.8319	7.5404	4.7963	4.0608	0.8014	1.9854
	Residual	0.2328	0.2670	0.2619	0.2467	0.2190	0.3327	0.4810	1.3505	1.4769
	$\|\|a\|\|$	0.2103	0.1573	0.1788	0.2560	0.1255	0.1879	0.8083	6.7276	7.3235
	$\|\|b\|\|$	73.594	68.030	67.018	67.370	60.633	43.724	39.062	8.5725	0.6492

(a)

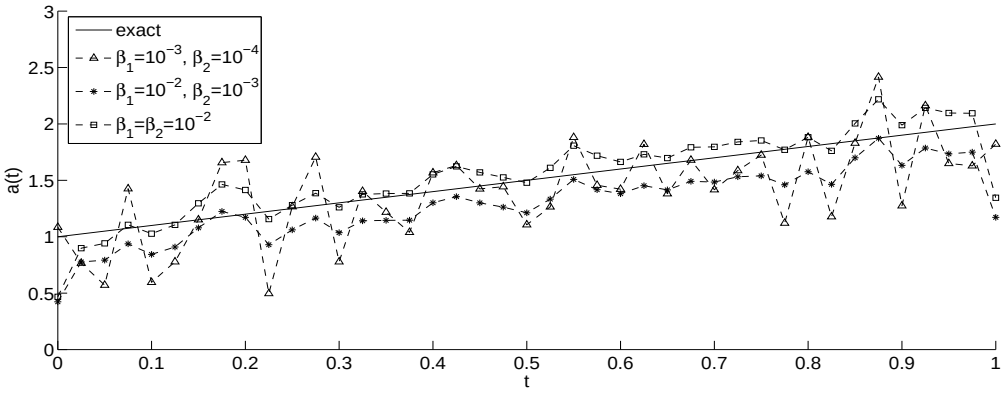

(b)

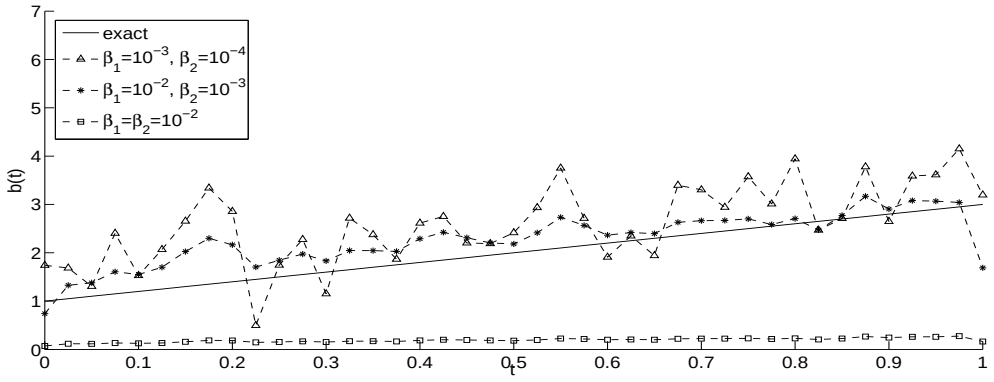

Figure 6: (a) Coefficient $a(t)$ and (b) Coefficient $b(t)$, for Example 1 with $p = 1\%$ noise and regularization.

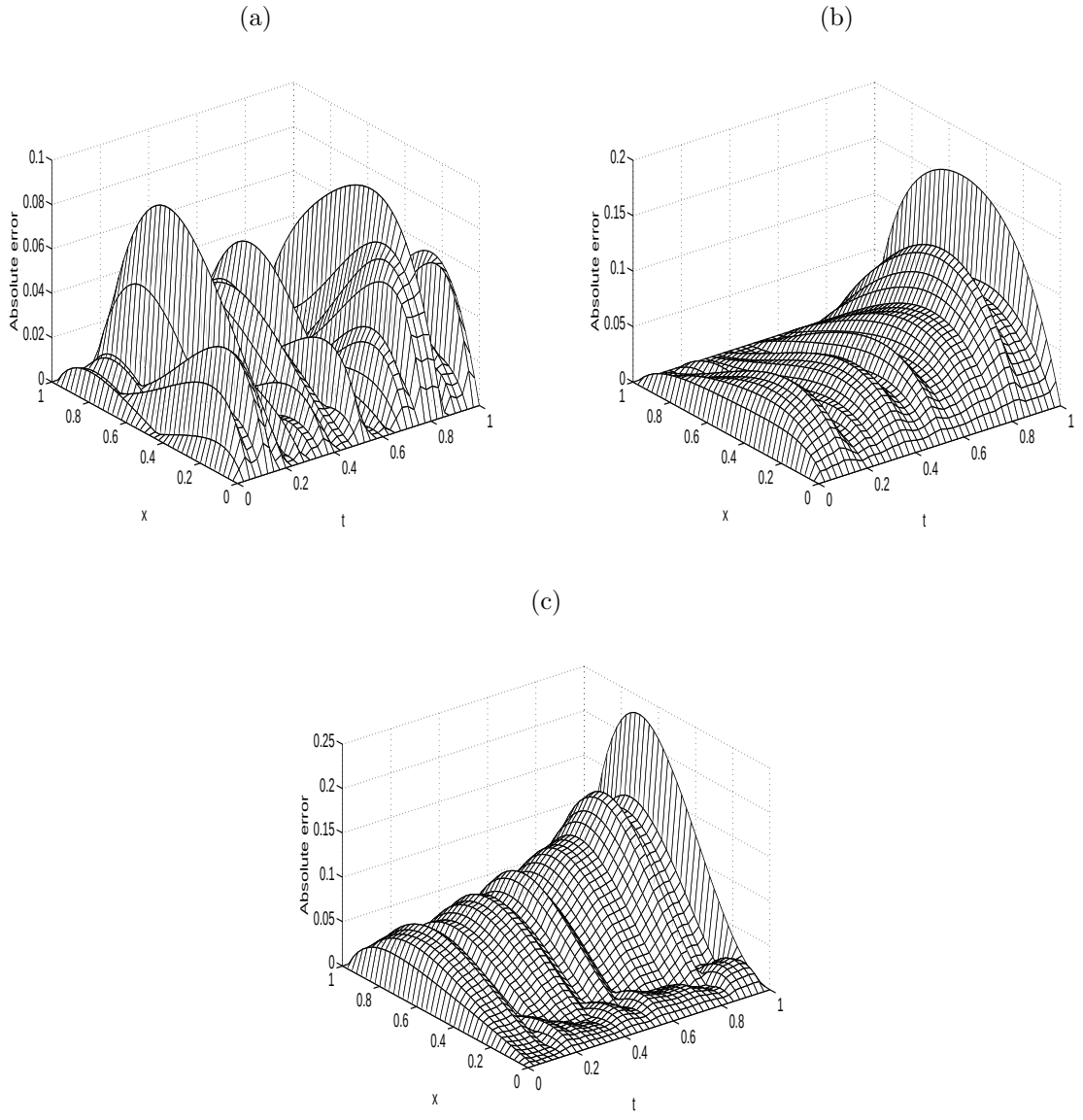

Figure 7: The absolute error between the exact and numerical temperatures $u(x,t)$, for Example 1, with (a) $\beta_1 = 10^{-3}$, $\beta_2 = 10^{-4}$, (b) $\beta_1 = 10^{-2}$, $\beta_2 = 10^{-3}$, (c) $\beta_1 = \beta_2 = 10^{-2}$, for $p = 1\%$ noise.

Example 2 (for IP1)

In this example, we consider the IP1 given by equations (2), (3), (5) and (6) with unknown coefficients $a(t)$ and $b(t)$ and we solve this inverse problem with the following input data:

$$\phi(x) = e^{-x} + x^2, \quad \mu_1(t) = e^t, \quad \mu_2(t) = (e^{-1}+1)e^t, \quad H_0(t) = \Big(-e^{-1} + \frac{4}{3}\Big)e^t,$$

$$H_1(t) = \Big(-2e^{-1} + \frac{5}{4}\Big)e^t, \quad T = L = 1,$$

$$f(x,t) = (e^{-x}+x^2)e^t - \Big(\Big|t-\frac{1}{2}\Big| + \frac{1}{2}\Big)(e^{-x}+2)e^t - \Big|t^2 - \frac{1}{2}\Big|(-e^{-x}+2x)e^t. \tag{43}$$

As for Example 1, the graph of the function $U_1(t)$ given by equation (7) is shown in Figure 2 and it can be seen that this function never vanishes over the time interval $t \in [0, 1]$. Hence, condition (7) is satisfied and consequently, according to Theorem 1, a solution to the IP1 given by equations (2), (3), (5) and (6) with the input data (43) is unique. In fact, the exact solution to the inverse problem is given by

$$a(t) = \left|t - \frac{1}{2}\right| + \frac{1}{2}, \quad b(t) = \left|t^2 - \frac{1}{2}\right|, \tag{44}$$

and $u(x, t)$ is given by (21).

Considering no noise and no regularization the objective function (34) plotted in Figure 3 shows a rapid decrease to a low value of $O(10^{-29})$ in 20 iterations. However, this convergence is slower than in Example 1 for the first 15 iterations. This is to be expected because the coefficients (20) for Example 1 are smoother than the coefficients (44) for Example 2. In Figure 8, we obtain a stable and accurate recovery of $a(t)$ but less stable for $b(t)$.

When $p = 0.01\%$ noise is included in the heat moments data (36), regularization is even more needed in order to achieve a stable and accurate solution. Table 3 shows the $rmse(a)$ and $rmse(b)$ for some values of the regularization parameters β_1 and β_2. Figure 9 shows the plots of the recovered coefficients $a(t)$ and $b(t)$. From both Table 3 and Figure 9 it can be seen that the retrieval of the thermal conductivity coefficient $a(t)$ is more stable and accurate than that of the convective coefficient $b(t)$.

Finally, we mention that a comparison between Figures 8 and 9, and Figures 22 and 24 of [6], respectively, shows that the IP1 based on measuring the heat moments (5) is less stable than when measuring the heat fluxes (4). This is to be expected since supplying the bounded normal derivatives (4) contains stronger information than prescribing the integral average heat moments (5).

In the next two examples we consider solving the IP2 formulated in subsection 2.2.

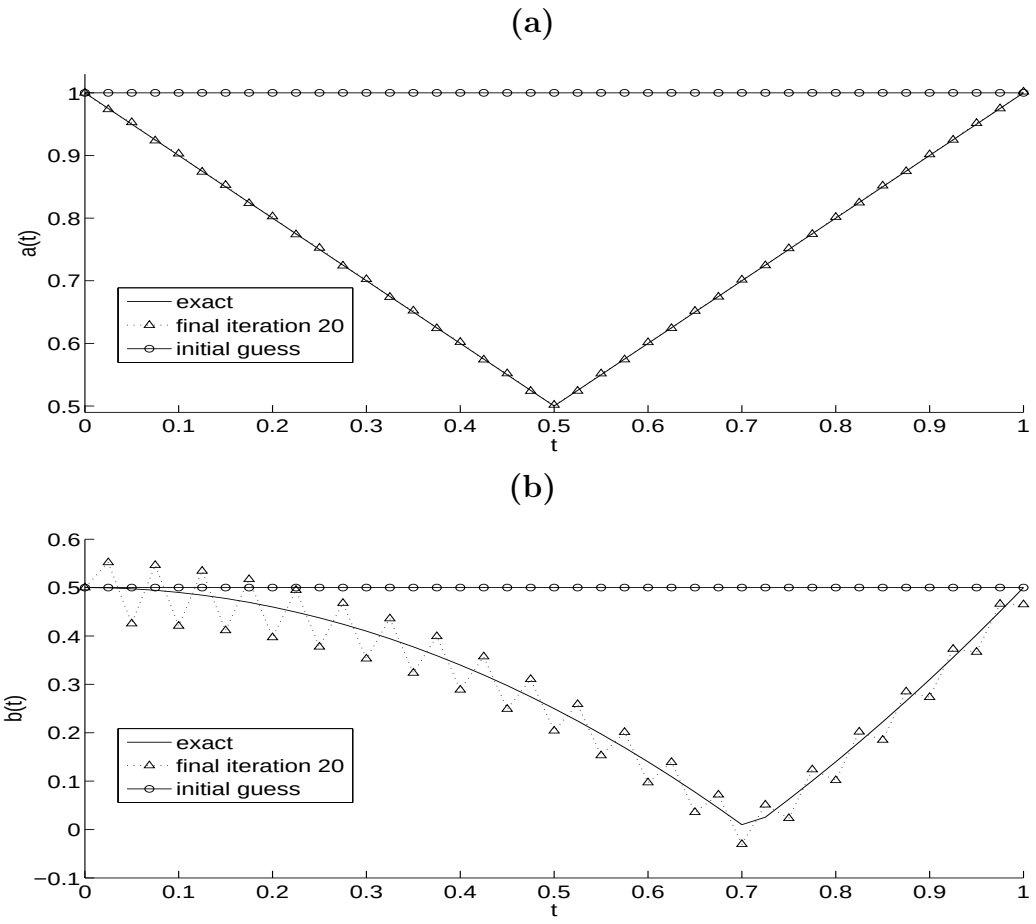

Figure 8: (a) Coefficient $a(t)$ and (b) Coefficient $b(t)$, for Example 2 with no noise and no regularization.

Table 3: The $rmse$ values for estimated coefficients for Example 2 with and without noise.

$rmse$	$p = 0$ $(\beta_1 = \beta_2 = 0)$	$p = 0.01\%$ $(\beta_1 = \beta_2 = 0)$	$p = 0.01\%$ $(\beta_1 = \beta_2 = 10^{-6})$
$rmse(a)$	0.0016	0.0830	0.0250
$rmse(b)$	0.0434	0.5360	0.0677

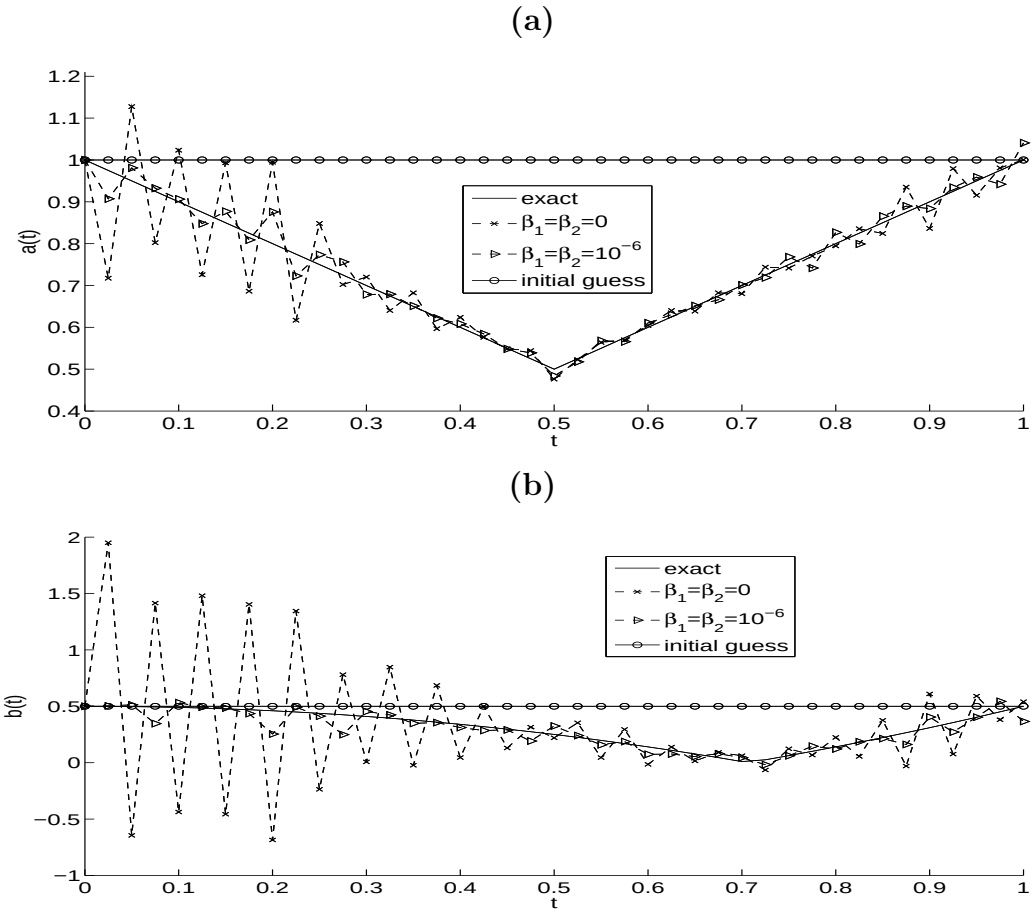

Figure 9: (a) Coefficient $a(t)$ and (b) Coefficient $b(t)$, for Example 2 with $p = 0.01\%$ noise, with and without regularization.

Example 3 (for IP2)

In this example, we consider the IP2 given by equations (2), (3), (5) and (9) with unknown coefficients $a(t)$ and $c(t)$ and solve this inverse problem with the following input data:

$$\phi(x) = (-2+x)^2, \quad \mu_1(t) = (-2+t)^2 + t, \quad \mu_2(t) = (-1+t)^2 + t, \quad H_0(t) = t^2 - 2t + \frac{7}{3},$$

$$H_1(t) = \frac{1}{12}\Big(6t^2 - 10t + 11\Big), \quad f(x,t) = 1 - 2(1+t) + 2(-2+x+t)$$
$$-(1+t)\Big(t + (-2+x+t)^2\Big), \quad T = L = 1. \tag{45}$$

The graph of the function $U_2(t)$ given by equation (10) is shown in Figure 10 and it can be seen that this function never vanishes over the time interval $t \in [0,1]$. Hence, condition (10) is satisfied and consequently, according to Theorem 2, a solution to the IP2 given by equations (2), (3), (5) and (9) with input data (45) is unique. In fact, this solution is given by

$$a(t) = 1 + t, \quad c(t) = 1 + t, \tag{46}$$

$$u(x,t) = (x + t - 2)^2 + t. \tag{47}$$

First, we consider the case that there is no noise in the input data (5). The convergence of the objective function (35) that is minimized with and without regularization is shown in Figure 11 and the corresponding numerical reconstructions of the coefficients $a(t)$ and $c(t)$ are shown in Figure 12. We also obtain the $rmse$ values of $rmse(a) \in \{0.0775, 0.1195\}$ and $rmse(c) \in \{0.1007, 0.1522\}$ with regularization $\beta_1 = 10^{-7}, \beta_2 = 10^{-9}$ and without regularization $\beta_1 = \beta_2 = 0$, respectively. Unlike the Example 1 for IP1, where no regularization was needed for exact data, in this Example 3 for IP2 the numerical results shown in Figure 12 and the decrease in the $rmse$ values reported above show that including a little regularization in (35) improves the accuracy and stability of the solution. It also shows that the IP2 is more ill-posed than the IP1.

To show this ill-posedness more dearly next we perturb the input data (5) by $p = 0.01\%$ noise as in equation (36). Figures 13 and 14 for this noisy data are the analogous of Figures 11 and 12 for exact data. We also report the values of $rmse(a) \in \{0.0719, 0.2489\}$ and $rmse(c) \in \{0.1025, 0.3709\}$ with regularization $\beta_1 = \beta_2 = 10^{-7}$ and without regularization $\beta_1 = \beta_2 = 0$, respectively. From these figures and $rmse$ values one can observe that the IP2 is ill-posed and regularization should be included in order to obtain a stable solution. The results also show that the IP2 is more ill-posed in the absorption coefficient $c(t)$ than in the diffusion coefficient $a(t)$.

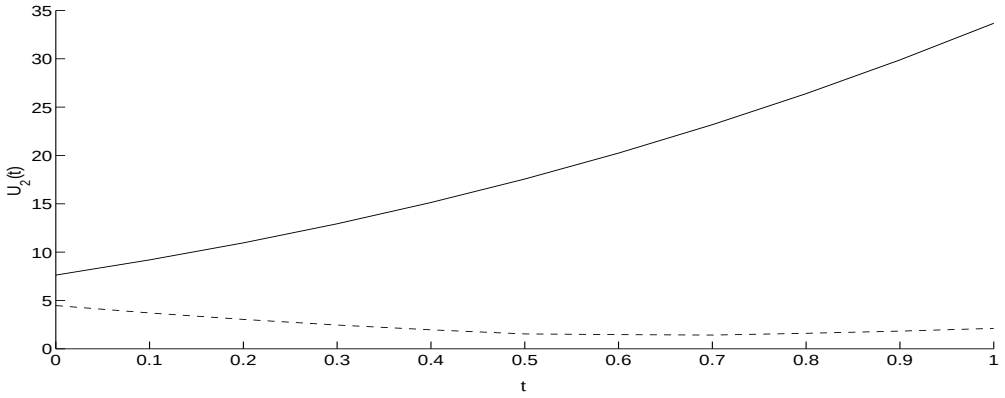

Figure 10: The graph of the function $U_2(t)$, as a function of t, given by (10) for Example 3 (——) and Example 4 (– – –).

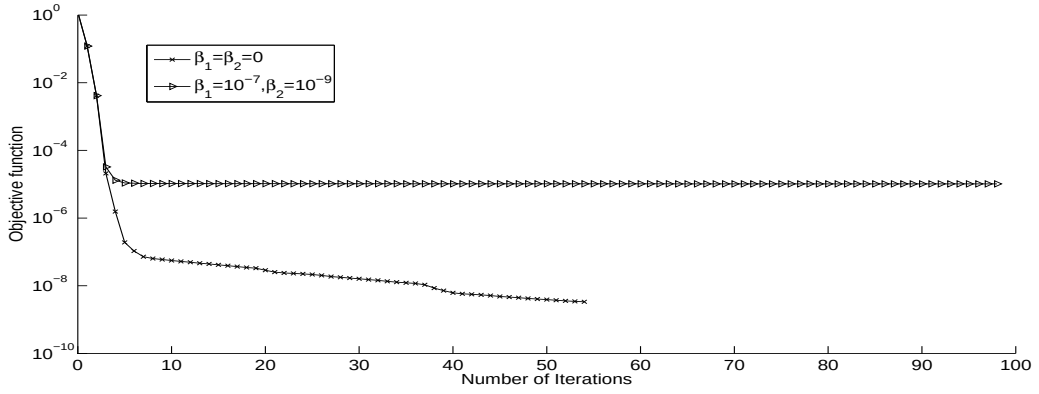

Figure 11: Objective function (35), for Example 3 with no noise, and with and without regularization.

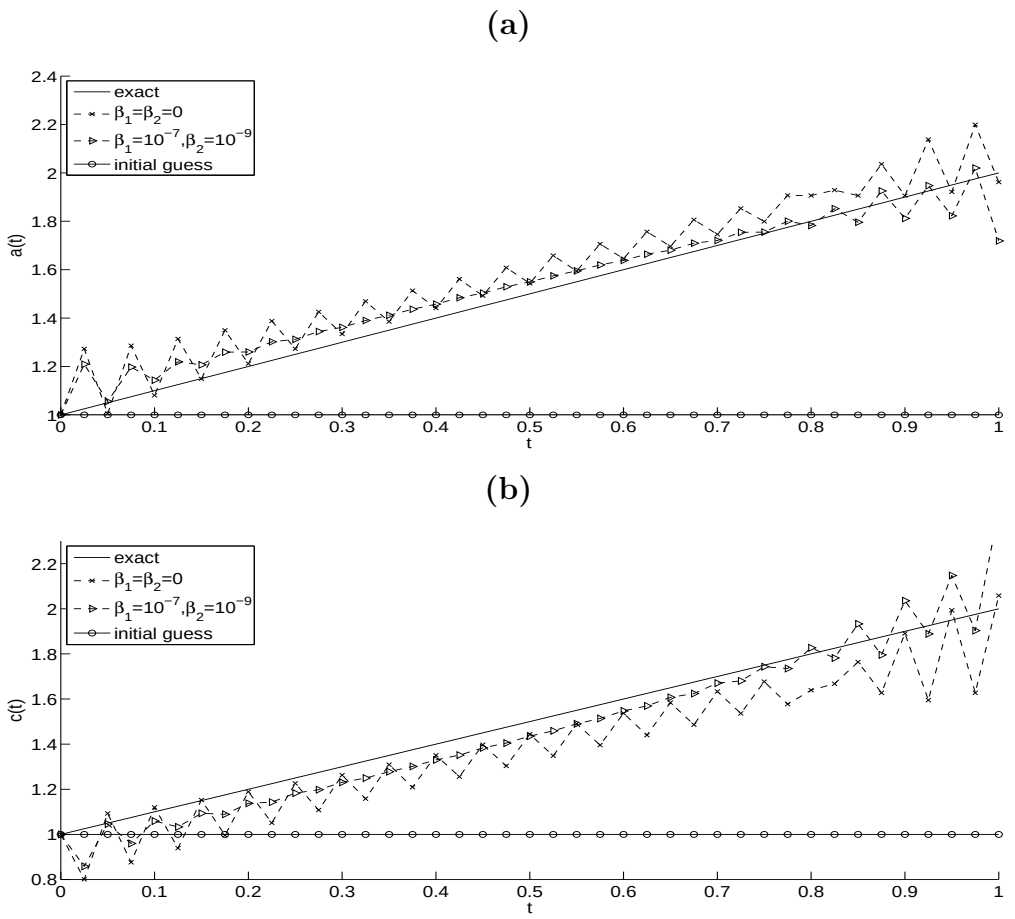

Figure 12: (a) Coefficient $a(t)$ and (b) Coefficient $c(t)$, for Example 3 with no noise, and with and without regularization.

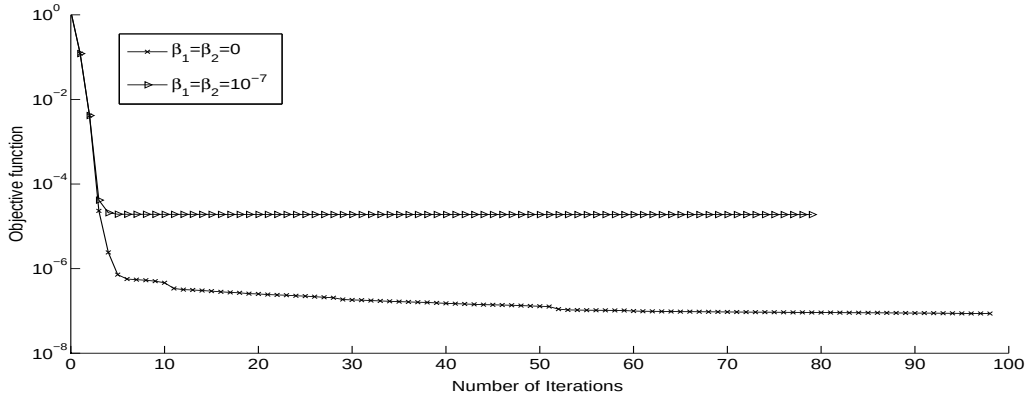

Figure 13: Objective function (35), for Example 3 with $p = 0.01\%$ noise, with and without regularization.

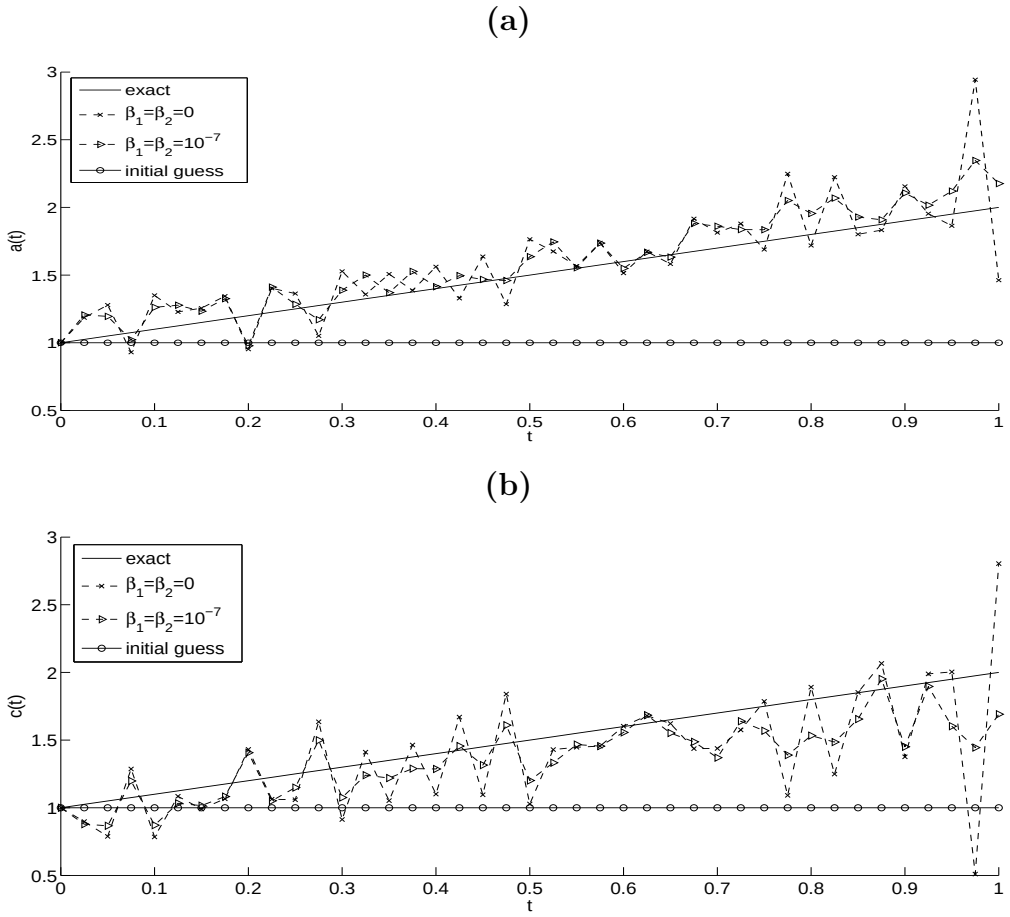

Figure 14: (a) Coefficient $a(t)$ and (b) Coefficient $c(t)$, for Example 3 with $p = 0.01\%$ noise, with and without regularization.

Example 4 (for IP2)

In this example, we consider the IP2 given by equations (2), (3), (5) and (9) with unknown coefficients $a(t)$ and $c(t)$ and we solve this inverse problem with the following input data:

$$\phi(x) = (-2+x)^2, \quad \mu_1(t) = (-2+t)^2 + t, \quad \mu_2(t) = (-1+t)^2 + t, \quad H_0(t) = t^2 - 2t + \frac{7}{3},$$
$$H_1(t) = \frac{1}{12}\Big(6t^2 - 10t + 11\Big), \quad f(x,t) = 1 + 2(-2+t+x) - 2\Big(\Big|t - \frac{1}{2}\Big| + \frac{1}{2}\Big)$$
$$-\Big(t + (-2+x+t)^2\Big)\Big(\Big|t^2 - \frac{1}{2}\Big| + \frac{1}{2}\Big), \quad T = L = 1. \tag{48}$$

As in Example 3, the function $U_2(t)$, given by equation (10) and plotted in Figure 10, never vanishes over the time interval $t \in [0,1]$ and consequently, the IP2 given by equations (2), (3), (5) and (9) with data (48) has at most one solution. In fact, this solution is given by

$$a(t) = \Big|t - \frac{1}{2}\Big| + \frac{1}{2}, \quad c(t) = \Big|t^2 - \frac{1}{2}\Big| + \frac{1}{2}, \tag{49}$$

and $u(x,t)$ given by (47).

Figures 15–18 for Example 4 are the analogous of Figures 11–14 for Example 3. For exact data, we also obtain $rmse(a) \in \{0.0579, 0.0756\}$ and $rmse(c) \in \{0.0690, 0.0890\}$

with regurarization $\beta_1 = \beta_2 = 10^{-7}$ and without regularization $\beta_1 = \beta_2 = 0$, respectively.

Similar conclusions to those obtained for Example 3 are also obtained for Example 4.

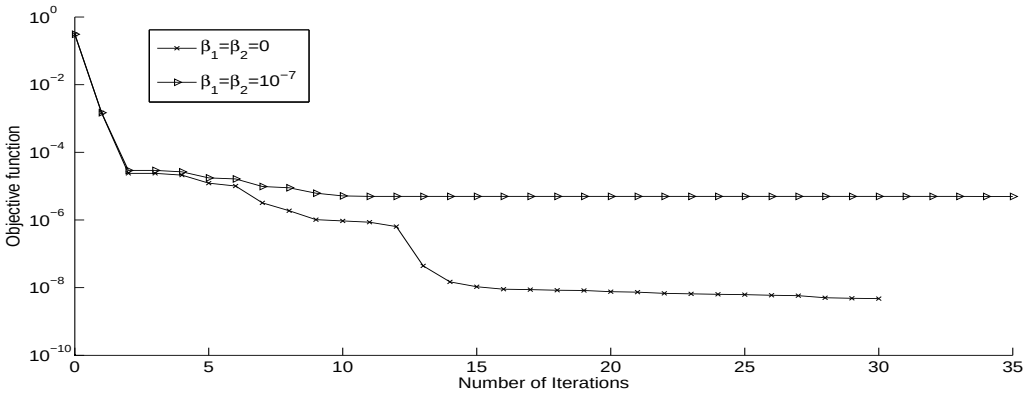

Figure 15: Objective function (35), for Example 4 with no noise, and with and without regularization.

(a)

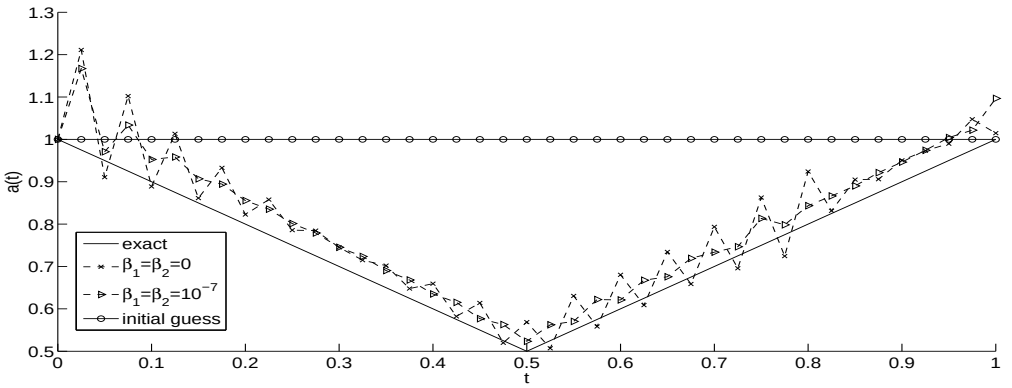

(b)

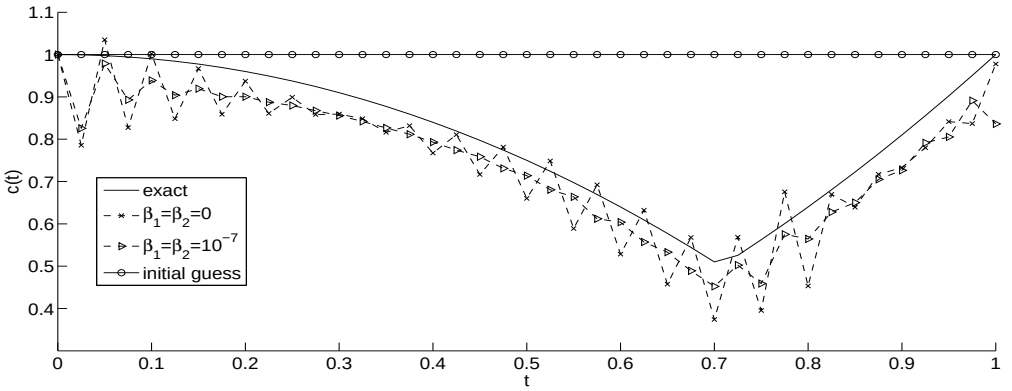

Figure 16: (a) Coefficient $a(t)$ and (b) Coefficient $c(t)$, for Example 4 with no noise, and with and without regularization.

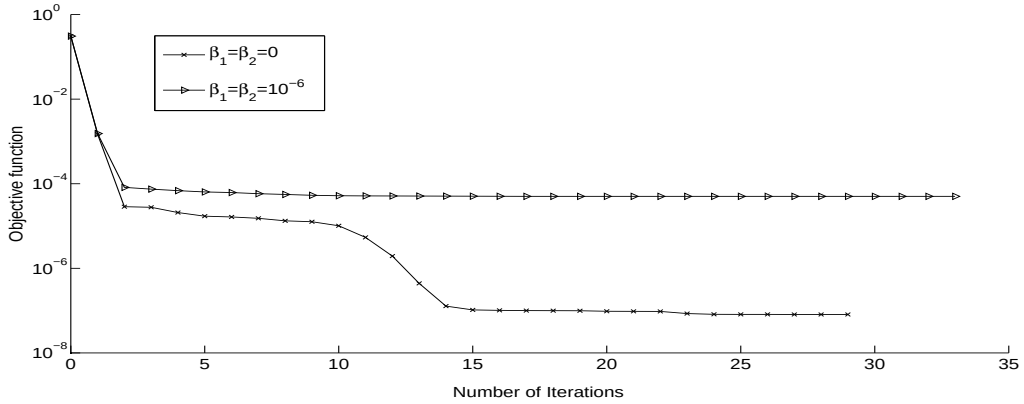

Figure 17: Objective function (35), for Example 4 with $p = 0.01\%$ noise, with and without regularization.

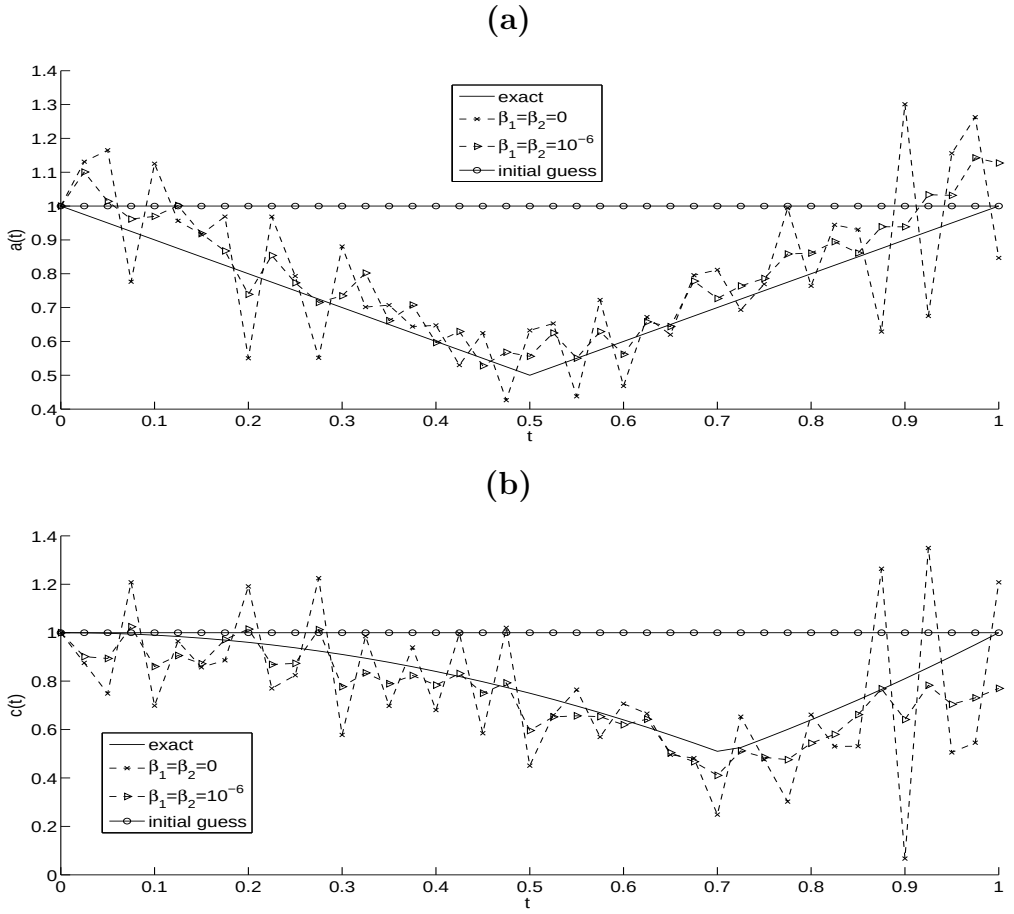

Figure 18: (a) Coefficient $a(t)$ and (b) Coefficient $c(t)$, for Example 4 with $p = 0.01\%$ noise, with and without regularization.

6 Conclusions

This paper has presented a simultaneous determination of time-dependent thermal conductivity and convection, or absorption coefficients from the measurements of the heat

moments in the one-dimensional parabolic heat equation. The resulting inverse problems have been reformulated as constrained regularized minimization problems which have been solved using the MATLAB optimization toolbox routine *lsqnonlin*. The following conclusions can be made:
• the numerical results are shown to be stable and accurate
• the IP2 seems more ill-posed that the IP1
• the retrieval of the diffusivity $a(t)$ is more stable and accurate than the retrieval of the lower-order coefficients $b(t)$ or $c(t)$
• the measurement of the heat moments (5) formulates a less stable inverse problem than the measurement of the heat fluxes (4).

The determination of three or more unknown coefficients in equation (1) will be investigated in a future work.

Acknowledgments

M.J. Huntul would like to thank Jazan University in Saudi Arabia and United Kingdom Saudi Arabian Cultural Bureau (UKSACB) in London for supporting his PhD at the University of Leeds. M.S. Hussein would like to thank the University of Leeds for hospitality.

References

[1] Belge, M., Kilmer, M. and Miller, E. (2002) Efficient determination of multiple regularization parameters in a generalized L-curve framework, *Inverse Problems*, **18**, 1161–1183.

[2] Cannon, J.R., Lin, Y. and Wang, S. (1991) Determination of a control parameter in a parabolic partial differential equation, *Journal of the Australian Mathematical Society, Series B,* **33**, 149–163.

[3] Coleman, T.F. and Li, Y. (1996) An interior trust region approach for nonlinear minimization subject to bounds, *SIAM Journal on Optimization*, **6**, 418–445.

[4] Fornasier, M., Naumova, V. and Pereverzyev, S.V. (2014) Parameter choice strategies for multipenalty regularization, *SIAM Journal on Numerical Analysis*, **52**, 1770–1794.

[5] Hansen, P.C. (1992) Analysis of discrete ill-posed problems by means of the L-curve. *SIAM Review,* **34**, 561–580.

[6] Hussein, M.S, Lesnic, D. and Ivanchov, M.I. (2014) Simultaneous determination of time-dependent coefficients in the heat equation, *Computers and Mathematics with Applications*, **67**, 1065–1091.

[7] Hussein, M.S. and Lesnic, D. (2016) Simultaneous determination of time and space-dependent coefficients in a parabolic equation, *Communications in Nonlinear Science and Numerical Simulations,* **33**, 194–217.

[8] Ivanchov, M.I. and Pabyrivs'ka, N.V. (2001) Simultaneous determination of two coefficients of a parabolic equation in the case of nonlocal and integral conditions, *Ukrainian Mathematical Journal*, **53**, 674–684.

[9] Ivanchov, N.I. and Pabyrivs'ka, N.V. (2002) On determination of two time-dependent coefficients in a parabolic equation, *Siberian Mathematical Journal*, **43**, 323–329.

[10] Lu, S. and Pereverzev, S.V. (2011) Multi-parameter regularization and its numerical realization, *Numerische Mathematik*, **118**, 1–31.

[11] Muzylev, N.V. (1983) On the uniqueness of the simultaneous determination of thermal conductivity and volume heat capacity, *USSR Computational Mathematics and Mathematical Physics*, **23**, 69–73.

[12] Mathwoks R2012 Documentation Optimization Toolbox-Least Squares (Model Fitting) Algorithms, available from www.mathworks.com/help/toolbox/optim/ug /brnoybu.html.

[13] Pabyrivs'ka, N. (2000) Integral conditions in an inverse problem for a parabolic equation, *Visnyk Lviv Univ. Ser. Mech. - Math.*, **56**, 142–149.

[14] Smith, G.D. (1985) *Numerical Solution of Partial Differential Equations: Finite Difference Methods*, Oxford Applied Mathematics and Computing Science Series, Third edition.

[15] Trucu, D., Ingham, D.B. and Lesnic, D. (2008) Inverse time-dependent perfusion coefficient identification, *Journal of Physics: Conference Series,* **124**, 012050 (28 pp).